PROCEEDINGS OF SPIE

SPIEDigitalLibrary.org/conference-proceedings-of-spie

Towards diode-pumped mid-infrared praseodymium-ytterbium-doped fluoride fiber lasers

R. I. Woodward, D. D. Hudson, S. D. Jackson

R. I. Woodward, D. D. Hudson, S. D. Jackson, "Towards diode-pumped mid-infrared praseodymium-ytterbium-doped fluoride fiber lasers," Proc. SPIE 10512, Fiber Lasers XV: Technology and Systems, 105120S (26 February 2018); doi: 10.1117/12.2294508

SPIE.

Event: SPIE LASE, 2018, San Francisco, California, United States

Towards diode-pumped mid-infrared praseodymium-ytterbium-doped fluoride fiber lasers

R. I. Woodward*, D. D. Hudson and S. D. Jackson

MQ Photonics Research Centre, Macquarie University
New South Wales, Australia

ABSTRACT

We explore the potential of a new mid-infrared laser transition in praseodymium-doped fluoride fiber for emission around 3.4 μm, which can be conveniently pumped by 0.975 μm diodes via ytterbium sensitizer co-doping. Optimal cavity designs are determined through spectroscopic measurements and numerical modeling, suggesting that practical diode-pumped watt-level mid-infrared fiber sources beyond 3 μm could be achieved.

Keywords: fiber lasers, rare-earth-doped gain media, zblan fiber, mid-infrared lasers, lanthanide spectroscopy

1. INTRODUCTION

There have been significant developments in mid-infrared (mid-IR) fiber lasers in recent years,[1] leading to demonstrations of fluoride fiber-based continuous wave (CW) sources with tens of watts average output powers[2] and ultrafast lasers producing pulses as short as 70 fs, with tens of kilowatts peak powers.[3] These devices have primarily been based on erbium- and holmium-doped ZBLAN fibers, emitting around 2.8 μm. Strong demand exists, however, to push the wavelength of such high-brightness sources further into the mid-IR, in order to enable new medical, sensing and manufacturing applications, due to the existence of strong absorption resonances beyond 3 μm for many important organic and technical materials.

To reach these longer wavelengths, alternative rare-earth dopants and transitions must be considered. For example, a dysprosium-doped fiber laser[4] has recently been demonstrated to lase up to 3.38 μm[5] (with nearly 600 nm tunability) and watt-level powers[6] have been generated from a ∼3.5 μm transition in erbium ZBLAN,[7] although this required a complex dual-wavelength pump scheme.[8] It should also be noted that there is intense research interest in rare-earth-doped chalcogenide fibers, which offer a wider transparency window and lower phonon energy than fluoride hosts,[9–11] although to date, it has not been possible to achieve mid-IR lasing in doped chalcogenide fiber, possibly due to impurity non-radiative relaxation effects.[9] Here, we propose and numerically explore a new route to longer wavelength mid-IR fiber lasers using praseodymium (Pr^{3+}) doped ZBLAN, conveniently diode-pumped via ytterbium (Yb^{3+}) co-doping.

2. MID-INFRARED EMISSION FROM PRASEODYMIUM-DOPED ZBLAN

Recent spectroscopic measurements revealed that the $^1G_4 \rightarrow {}^3F_4$ transition in Pr^{3+}:ZBLAN (illustrated schematically in Fig. 1) offers a broad emission cross section spanning ∼3.1 to 3.9 μm (Fig. 2), with ∼70 μs upper state lifetime and a branching ratio of 0.05.[12] This is a four-level laser transition with fast de-excitation of the lower level by multiphonon relaxation (MPR). To overcome the weak absorption cross section at 1.01 μm ($\sim 0.4\times10^{-25}$ m^2) that is required to populate the $^1G_4$ level, the glass can be co-doped with Yb^{3+} sensitizer, which offers strong absorption at 0.975 μm ($\sim 8\times10^{-25}$ m^2, as shown in Fig. 3). The $^1G_4$ manifold in praseodymium is then populated by an efficient energy transfer (ET) process from ytterbium: Yb^{3+}:$^2F_{5/2} \rightarrow Pr^{3+}$:$^1G_4$ (the backward ET process is weak).

This sensitization approach has previously been successfully applied for the development of 1.3 μm Pr^{3+} ZBLAN fibre amplifiers for telecommunication applications,[13] based on the $^1G_4 \rightarrow {}^3H_5$ transition which shares the same upper state as the ∼3.5 μm transition of interest in this work. The ability to pump this transition

*robert.woodward@mq.edu.au

Fiber Lasers XV: Technology and Systems, edited by Ingmar Hartl, Adrian L. Carter, Proc. of SPIE
Vol. 10512, 105120S · © 2018 SPIE · CCC code: 0277-786X/18/$18 · doi: 10.1117/12.2294508

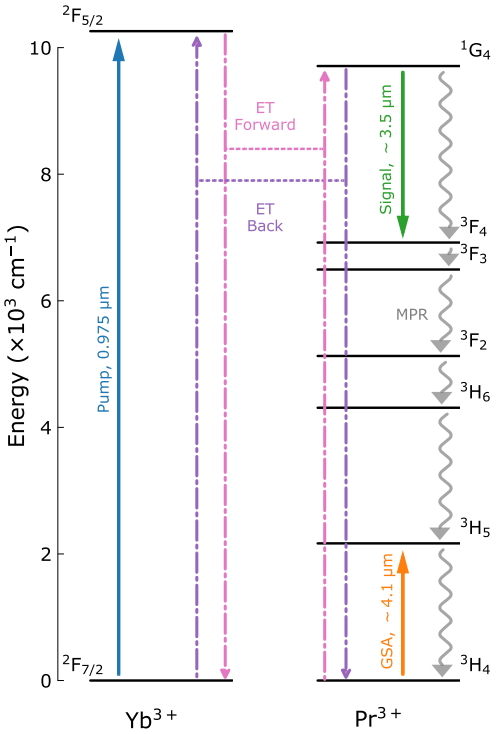

Figure 1. Energy levels for ytterbium and praseodymium, showing salient transitions for diode-pumped mid-IR emission, including energy transfer (ET) and non-radiative multiphonon relaxation (MPR).

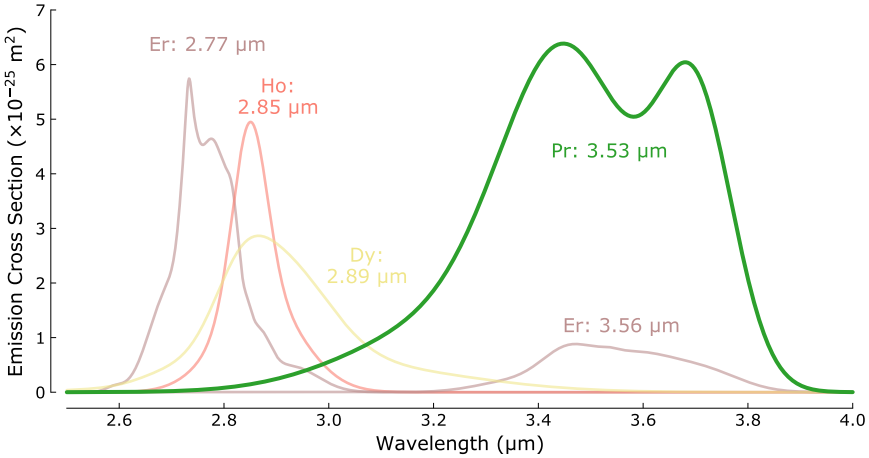

Figure 2. Effective emission cross sections for various rare-earth-doped ions suitable for mid-IR fibre laser development (with annotated central wavelength), including the new proposed praseodymium transition in this work.

using highly efficient high-power diodes that are commercially available is significant, improving the prospects for practical, efficient mid-IR lasers using this transition.

It should also be noted, however, that Pr^{3+}:ZBLAN exhibits a wide ground state absorption ($^3H_4 \rightarrow {}^3H_5$), which overlaps the emission from our proposed transition towards longer wavelengths (Fig. 4). This will result in reabsorption of the generated mid-IR light, impacting upon the overall efficiency. Therefore, to evaluate the prospect of mid-IR $Pr^{3+}Yb^{3+}$ lasers, we develop a comprehensive numerical model including atomic population and optical power dynamics for all relevant transitions (also including ASE and competing emission at 1 & 1.3 µm).

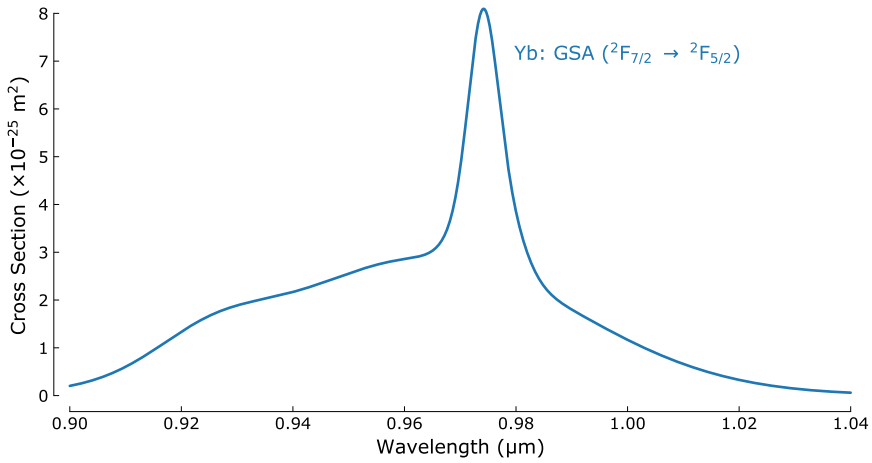

Figure 3. Effective ground-state absorption (GSA) cross section for ytterbium:ZBLAN. Adapted from Ref.[14]

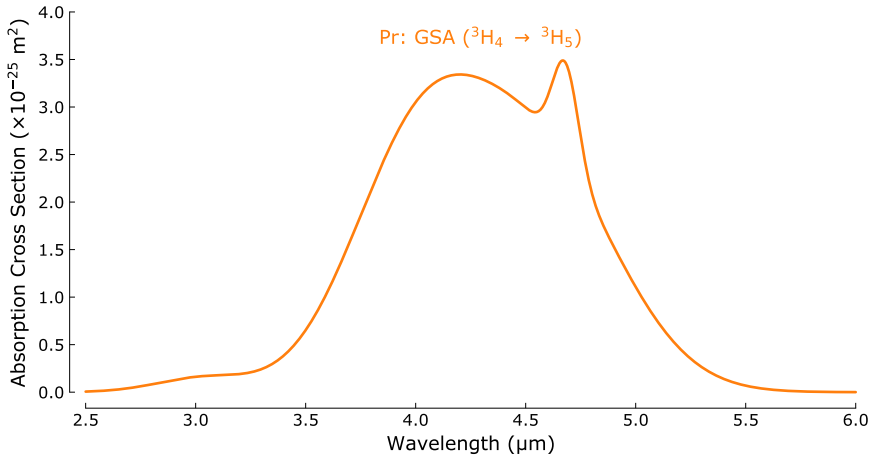

Figure 4. Effective ground-state absorption (GSA) cross section measured for praseodymium:ZBLAN.

3. NUMERICAL METHODS

Briefly, a rate equation model is developed where the power evolution $P(z)$ along the doped fiber (with longitudinal co-ordinate z) for each spectral channel of wavelength λ is governed by:

$$\frac{\mathrm{d}P(\lambda,z)}{\mathrm{d}z} = \pm\left(P(\lambda,z)\left(\Gamma(\lambda)\left[\sum_{j,k}\sigma_{kj}(\lambda)N_k(z) - \sigma_{jk}(\lambda)N_j(z)\right] - l\right) + P_{\mathrm{spon}}(\lambda)\right) \tag{1}$$

where Γ is the core overlap factor, σ_{ij} is the $i \to j$ cross section, l is the background loss (a typical constant value of 0.1 dB/m for fluoride fiber is assumed here). Spontaneous emission P_{spon} is included using the standard approach,[15] for many spontaneous emission channels (with spectral width Δf):

$$P_{\mathrm{spon}}(\lambda) = \Gamma(\lambda)\left(\sum_{\substack{i,j \\ i>j}}\sigma_{ij}(\lambda)N_i(z)\right)\frac{hc\Delta f}{\lambda}. \tag{2}$$

The atomic level populations for all m levels $\mathbf{N} = [N_0, N_1 ... N_m]$ are governed by rate equations at each z

position, expressed in matrix notation as:

$$\frac{\mathrm{d}\mathbf{N}}{\mathrm{d}t} = \begin{bmatrix} -\sum_{i=0}^{m} R_{0i} & \cdots & R_{m0} \\ \vdots & \ddots & \vdots \\ R_{0m} & \cdots & -\sum_{i=0}^{m} R_{mi} \end{bmatrix} \mathbf{N} + \begin{bmatrix} \sum_{k=0 \text{ or } l=0}^{i,j,k,l} k_{ijkl} N_i N_j - \sum_{i=0 \text{ or } j=0}^{i,j,k,l} k_{ijkl} N_i N_j \\ \vdots \\ \sum_{k=m \text{ or } l=m}^{i,j,k,l} k_{ijkl} N_i N_j - \sum_{i=m \text{ or } j=m}^{i,j,k,l} k_{ijkl} N_i N_j \end{bmatrix} \tag{3}$$

where the linear population change rate terms are:

$$R_{ij} = \underbrace{\beta_{ij}/\tau_i}_{\text{radiative relaxation}} + \underbrace{C(T)\exp(-\alpha \Delta E_{ij})}_{\text{nonradiative relaxation}} + \underbrace{\sum_{\lambda} \sigma_{ij}(\lambda) \frac{P(\lambda)\Gamma}{A_{\text{core}} \times hc/\lambda}}_{\text{stimulated abs. / emis.}} \tag{4}$$

and k_{ijkl} is the energy transfer coefficient for the interionic process: $i \rightarrow k$ & $j \rightarrow l$, and A_{core} is the doped core area. Spectroscopic parameters (at room temperature, $T = 300$ K) including branching ratios β, radiative lifetimes τ and multiphonon decay constants (C & α, based on a standard energy gap law) are obtained from direct measurement, Judd-Ofelt analysis or literature.[12] The system of equations is solved for the steady state $\mathrm{d}\mathbf{N}/\mathrm{d}t = 0$ using a fourth-order collocation algorithm to identify a self-consistent evolution of power values along the fiber, subject to our chosen boundary conditions (i.e. cavity mirror reflectivity values). All numerical modeling is performed using Python (with Scientific Python SciPy libraries[16]).

4. RESULTS AND DISCUSSION

We consider a linear cavity (Fig. 5) with Yb^{3+}(1 mol%)Pr^{3+}(1 mol%)-doped double-clad ZBLAN fiber (15 μm core diameter and 0.16 NA; 240 μm cladding diameter). A narrowband dichroic cavity mirror (100% reflective for the signal and highly transmissive for the pump) and a 4% reflective cleaved fiber end are used to form the cavity, and we note that with ongoing developments in fluoride fiber components, this could also be simply implemented using a fiber Bragg grating,[17,18] or a ring cavity with a fused-fiber coupler.[19]

To identify optimal lengths / potential operating wavelengths, we perform an ensemble of simulations to determine lasing thresholds, with the results visualized in Fig. 6(a). The lowest thresholds occur around 3.3–3.4 μm with 0.5–1.0 m fiber lengths. Unfortunately, despite the broad emission cross section, a sharp increase in thresholds beyond ~3.6 μm is noted, highlighting the negative impact of ground state absorption (Fig. 4) that may prevent full exploitation of the emission bandwidth.

Despite this limitation, our calculated threshold values suggest valid opportunities for $Pr^{3+}Yb^{3+}$-doped fluoride fiber lasers beyond 3 μm. An example cavity is considered with 0.5 m fiber length and a mirror with 100% reflectivity at 3.4 μm (the other end is simply planar cleaved to give a broadband 4% reflection). Our simulation indicates that lasing will occur at an incident pump threshold of ~13 W with 2.9% slope efficiency (Fig. 7), corresponding to 4.4 W threshold and 9.3% slope efficiency in terms of absorbed pump power.

With 50 W launched pump power, which is readily accessible at 0.975 μm from commercial diode lasers, and by varying the cavity mirror peak-reflectivity wavelength, we find that over 1 W CW power could be achieved

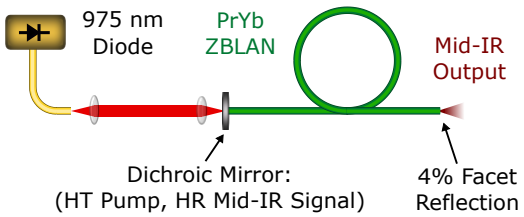

Figure 5. Cavity schematic for proposed diode-pumped mid-IR $Pr^{3+}Yb^{3+}$:ZBLAN fiber laser. The dichroic mirror (highly transmissive (HT) for the pump and highly reflective (HR) for the signal wavelength) is butt-coupled to the fiber.

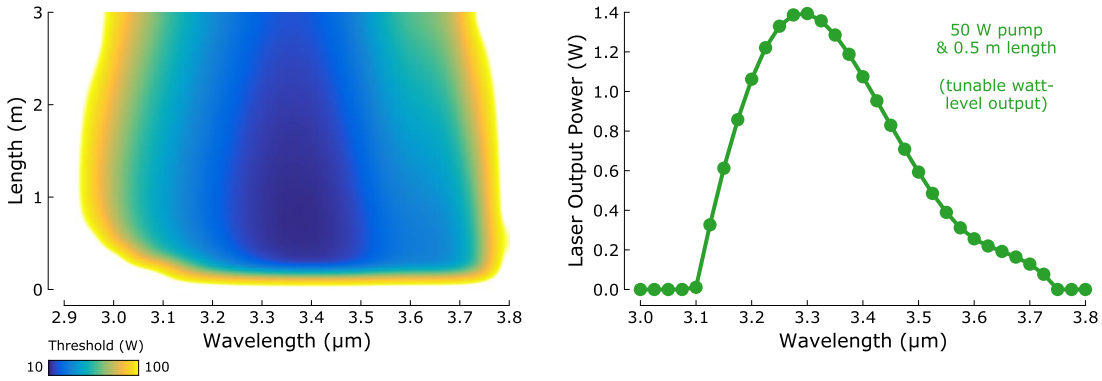

Figure 6. Calculated tunability from simulations: (a) lasing threshold as function of fiber length and lasing wavelength; (b) output power for 0.5 m length for varying lasing wavelength.

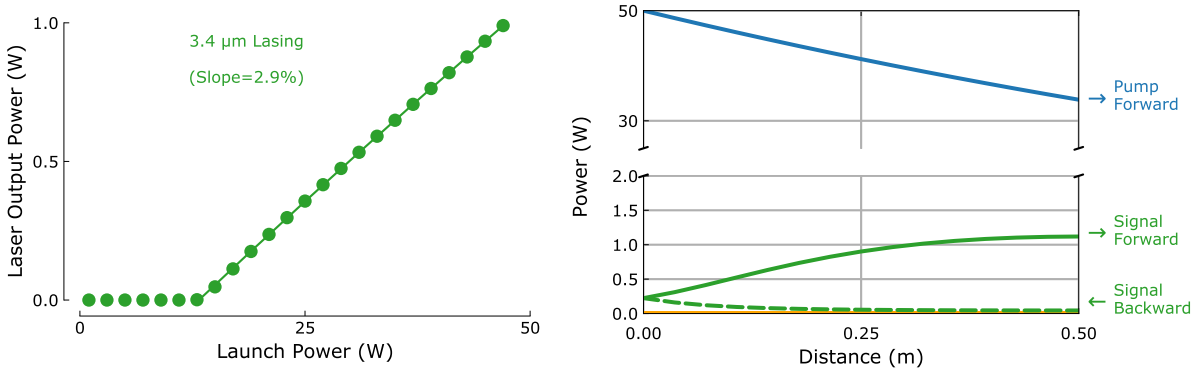

Figure 7. Simulation results for a $Pr^{3+}Yb^{3+}$:ZBLAN laser with 0.5 m length and a dichroic cavity mirror optimized for 3.4 μm wavelength: (a) power curve; (b) intracavity power evolution for 50 W pump power (ASE is included in the model, but is negligible here).

over a broad 250 nm tuning range centered at 3.3 μm [Fig. 6(b)]; this range includes the absorption peaks of many polymers, suggesting applications in advanced manufacturing. On a practical note, the multiphonon relaxation from the lower laser level ($^3F_4$) to the ground state ($^3H_4$) will cause heating of the fiber, hence it was designed with a large 240 μm inner cladding and we expect to be able to dissipate this heat with an air-cooled fiber mandrel.

5. CONCLUSION

In conclusion, we have proposed and numerically verified a route towards mid-IR fiber lasers beyond 3 μm by exploiting a previously unexplored transition in Pr^{3+}:ZBLAN. Spectroscopic measurements and numerical simulations were used to identified optimized cavity designs, suggesting watt-level emission over a broad 250 nm range is possible using currently available pump diode technology. A suitable $Pr^{3+}Yb^{3+}$ fluoride fiber has been fabricated and work is ongoing to experimentally demonstrate our proposed laser design.

ACKNOWLEDGMENTS

We thank Dr Laercio Gomes for access to spectroscopic data. RIW acknowledges support through an MQRF Fellowship.

REFERENCES

[1] Jackson, S. D., "Towards high-power mid-infrared emission from a fibre laser," *Nature Photon.* **6**(7), 423–431 (2012).

[2] Fortin, V., Bernier, M., Bah, S. T., and Vallee, R., "30 W fluoride glass all-fiber laser at 2.94 μm," *Opt. Lett.* **40**(12), 2882–2885 (2015).
[3] Woodward, R. I., Hudson, D. D., Fuerbach, A., and Jackson, S. D., "Generation of 70-fs pulses at 2.86 μm from a mid-infrared fiber laser," *Opt. Lett.* **42**(23), 4893 (2017).
[4] Jackson, S. D., "Continuous wave 2.9 μm dysprosium-doped fluoride fiber laser," *Appl. Phys. Lett.* **83**(7), 1316–1318 (2003).
[5] Majewski, M., Woodward, R. I., and Jackson, S. D., "Dysprosium-doped ZBLAN fiber laser tunable from 2.8 to 3.4 μm, pumped at 1.7 μm," *Submitted* (2017).
[6] Fortin, V., Maes, F., Bernier, M., Bah, S. T., D'Auteuil, M., and Vallée, R., "Watt-level erbium-doped all-fiber laser at 3.44 μm," *Opt. Lett.* **41**(3), 559 (2016).
[7] Tobben, H., "Room temperature CW fibre laser at 3.5 um in Er3+-doped ZBLAN glass," *Electron. Lett.* **28**(14), 1361–1362 (1992).
[8] Henderson-Sapir, O., Jackson, S. D., and Ottaway, D. J., "Versatile and widely tunable mid-infrared erbium doped ZBLAN fiber laser," *Opt. Lett.* **41**(7), 1676–1679 (2016).
[9] Seddon, A. B., Tang, Z., Furniss, D., Sujecki, S., and Benson, T. M., "Progress in rare-earth-doped mid-infrared fiber lasers," *Opt. Express* **18**(25), 26704–26719 (2010).
[10] Sakr, H., Tang, Z., Furniss, D., Sojka, L., Sujecki, S., Benson, T. M., and Seddon, A. B., "Promising emission behavior in Pr3+/In selenide-chalcogenide-glass small-core step index fiber (SIF)," *Opt. Mater.* **67**, 98–107 (2017).
[11] Liu, Z., Bian, J., Huang, Y., Xu, T., Wang, X., and Dai, S., "Fabrication and characterization of mid-infrared emission of Pr 3+ doped selenide chalcogenide glasses and fibres," *RSC Adv.* **7**(66), 41520–41526 (2017).
[12] Gomes, L. and Jackson, S. D., "Spectroscopic properties of ytterbium, praseodymium-codoped fluorozirconate glass for laser emission at 3.6 μm," *J. Opt. Soc. Am. B* **30**(6), 1410 (2013).
[13] Ohishi, Y., Kanamori, T., Temmyo, J., Wada, M., Yamada, M., Shimizu, M., Yoshino, K., Hanafusa, H., Horiguchi, M., and Takahashi, S., "Laser diode pumped Pr3+-doped and Pr3+-Yb3+-codoped fluoride fibre amplifiers operating at 1.3 um," *Electron. Lett.* **27**(22), 1995 (1991).
[14] da Vila, L. D., Gomes, L., Tarelho, L. V. G., Ribeiro, S. J. L., and Messadeq, Y., "Mechanism of the YbEr energy transfer in fluorozirconate glass," *J. Appl. Phys.* **93**(7), 3873 (2003).
[15] Giles, C. and Desurvire, E., "Modeling erbium-doped fiber amplifiers," *J. Light. Technol.* **9**(2), 271–283 (1991).
[16] Jones, E., Oliphant, T., and Peterson, P., "SciPy: Open source scientific tools for Python," (2001).
[17] Haboucha, A., Fortin, V., Bernier, M., Genest, J., Messaddeq, Y., and Vallée, R., "Fiber Bragg grating stabilization of a passively mode-locked 2.8 μm Er3+: fluoride glass fiber laser," *Opt. Lett.* **39**(11), 3294 (2014).
[18] Bharathan, G., Woodward, R. I., Ams, M., Hudson, D. D., Jackson, S. D., and Fuerbach, A., "Direct inscription of Bragg gratings into coated fluoride fibers for widely tunable and robust mid-infrared lasers," *Opt. Express* **25**(24), 30013 (2017).
[19] Stevens, G. and Woodbridge, T., "Mid-IR fused fiber couplers," *Proc. SPIE* **9730**, 973007 (2016).